Interactions Between Polymers and Liquids during Initiated Chemical Vapor Deposition onto Liquid Substrates

Journal:	*Molecular Systems Design & Engineering*
Manuscript ID	ME-REV-07-2019-000087.R1
Article Type:	Review Article
Date Submitted by the Author:	09-Sep-2019
Complete List of Authors:	De Luna, Mark; University of Southern California, Chemical Engineering and Materials Science Karandikar, Prathamesh; University of Southern California, Chemical Engineering and Materials Science Gupta, Malancha; University of Southern California, Chemical Engineering and Materials Science

Interactions Between Polymers and Liquids during Initiated Chemical Vapor Deposition onto Liquid Substrates

Mark M. De Luna, Prathamesh Karandikar, Malancha Gupta*

Mork Family Department of Chemical Engineering and Materials Science, University of Southern California, Los Angeles, California, 90089, U.S.A.

*Corresponding Author Email: malanchg@usc.edu

Abstract

Vapor phase deposition is typically used to apply thin films and coatings onto solid substrates. Deposition of materials onto liquid substrates provides complexity due to surface tension, viscosity, and solubility effects. Understanding the interactions between the deposited material and the liquid substrate can lead to the formation of materials with new structures and compositions. In this review, we will discuss the interactions associated with initiated chemical vapor deposition of polymers onto liquid substrates including silicone oils and ionic liquids. We will provide guidelines for selecting liquid properties to control the formation of polymer particles, films, and gels. We will conclude by discussing recent work on combining polymer and metal deposition to create hybrid organic/inorganic structures and actively moving the liquid during polymer deposition.

Design, System, Application

This review article highlights the interactions between the polymer and the liquid substrate during initiated chemical vapor deposition. Different polymer morphologies of varying length scales can be obtained including nanoparticles, films, and gels by selecting the surface tension of the polymer and liquid, the viscosity of the liquid, and the solubility of the monomer. The polymer deposition time can be varied to control the size of the particles and the thickness of the films. Ionic liquids can be incorporated into gels or encapsulated within polymer shells. We also highlight recent work that demonstrates that sputter deposition can combined with initiated chemical vapor deposition to fabricate hybrid organic/inorganic materials for potential applications in electronics and catalysis.

Introduction

The initiated chemical vapor deposition (iCVD) process is a solventless technique that can be used to deposit functional polymer coatings onto a variety of solid substrates.[1–3] In the iCVD process, monomer and initiator vapors are delivered continuously into a reactor that is kept at 50 – 500 mTorr. A heat exchanger is used to cool the substrate to a desired temperature typically between 20 – 40 ℃. The initiator molecules are thermally cleaved into free radicals by a nichrome filament array heated to 200 – 250 ℃, and these free radicals diffuse to the substrate. The concentration of monomer that adsorbs to the substrate can be increased by decreasing the substrate temperature,[4] increasing the monomer flow rate,[4,5] or increasing the reactor pressures.[4–6] Polymerization occurs via a classical free radical mechanism leading to average molecular weights ranging from 10,000 to 800,000 Da with typical PDIs of 1.7 - 2.6.[7–9] The solventless nature of the iCVD process allows for deposition of conformal polymer coatings onto substrates with complex geometries including microtrenches,[10–12] fibers,[13–15] membranes,[16–18] carbon nanotubes,[19,20] and microfluidic channels.[21,22]

The introduction of liquids as substrates during vapor phase deposition processes is complex due to a wide variety of possible interactions between the deposited material and the liquid. The liquid substrates must have low vapor pressures to prevent evaporation. A wide variety of liquids satisfy this criterion including ionic liquids, silicone oils, glycerol, squalene, and Krytox. Ionic liquids (ILs) are of particular interest because of their high ionic conductivity, thermal stability, and wide electrochemical window which allows for applications in energy storage, chemical synthesis, and gas absorption.[23–25] Silicone oils are an ideal substrate since they are nontoxic, have a range of viscosities, and are inert, which allows for studying the effects of liquid properties in the absence of chemical interactions. The vapor phase deposition of inorganic

materials onto liquid substrates via thermal evaporation and sputter deposition has been recently studied.[26–38] It was found that sputtering conditions,[39,40] liquid properties,[29,30] and the type of sputtered metal[32] can be varied to create structures such as ramified aggregates, nanoparticles, and films. These types of nanostructured materials have potential uses in catalysis and plasmonics.[41] The curved surface of liquid substrates is useful for fabricating mirrors and lenses. For example, chromium was deposited onto IL to fabricate a mirror for a lunar telescope.[32] The vapor phase deposition of organic materials onto liquid substrates has been studied less than inorganic deposition. The deposition of Parylene has been used for the encapsulation of liquids for use as intraocular lenses.[42,43,44] For example, a liquid lens with a tunable focal distance was fabricated by depositing Parylene onto a droplet of silicone oil.[44]

Our group demonstrated for the first time that iCVD can be used to deposit polymers onto liquid substrates in 2011.[45] This review paper will focus specifically on the interactions between the polymer and the liquid substrate during iCVD. We will highlight the different polymer morphologies of varying length scales that can be obtained by selecting the surface tension of the polymer and liquid, the viscosity of the liquid, and the solubility of the monomer. We will demonstrate the high throughput synthesis of polymer nanoparticles which can be useful for fabricating materials for drug delivery[46] and catalysis.[47] We will demonstrate that ionic liquids can be encapsulated within polymer shells or incorporated into gels. We will also show that sputter deposition can combined with initiated chemical vapor deposition to fabricate hybrid organic/inorganic materials which are potentially useful for applications in electronics,[48] drug delivery,[49] separations,[50] catalysis,[51] and environmental remediation.[52] Our review specifically focuses on iCVD deposition onto liquid substrates because the versatility of the process allows for systematic variation of different parameters. For example, the solubility of the system can be

varied by choosing different combinations of monomers and liquids and the surface energy of the deposited polymer can be varied from 20 to 60 mN/m which is not achievable for high surface energy materials such as metals.[30] The iCVD process also allows for systematic variation of the molecular weight of the polymer chains and the degree of crosslinking which allows the effects of diffusion and aggregation to be systematically studied. Although this review focuses on iCVD deposition onto liquids, the fundamental insight provided in this review can be applied to other deposition methods as we have recently shown in our sputtering studies.[30,53]

For our first demonstration of iCVD onto liquids, we studied the deposition of poly(1*H*,1*H*,2*H*,2*H*-perfluorodecyl acrylate) (PPFDA) and poly(2-hydroxyethyl methacrylate) (PHEMA) onto a droplet of 1-butyl-3-methylimidazolium hexafluorophosphate ([bmim][PF_6]).[45] We found that polymerization could either occur at the vapor-liquid interface or within the bulk of the liquid depending on the solubility of the monomer within the liquid. The solubility of the monomers in the liquids can be tested using an *in situ* quartz crystal microbalance (QCM). The monomer, 1*H*,1*H*,2*H*,2*H*-perfluorodecyl acrylate (PFDA), is not soluble in [bmim][PF_6] and therefore polymerization occurs only at the vapor-liquid interface whereas the monomer, 2-hydroxyethyl methacrylate (HEMA), is soluble within [bmim][PF_6] and therefore polymerization occurs at both the vapor-liquid interface and within the bulk liquid. In this review paper, we will discuss the different structures that can be formed for insoluble[45,54–59] and soluble systems[8,45,54,60,61] as shown in Figure 1. For the case of insoluble monomers, the structures formed at the vapor-liquid interface are composed only of polymer whereas for the case of soluble systems, the liquid is incorporated into the final structure.

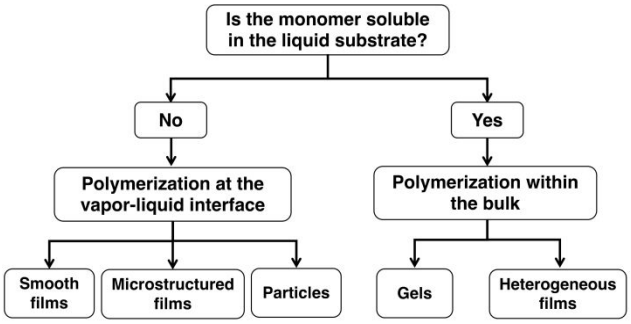

Figure 1 – Flow diagram of different structures that can be formed for cases where the monomer is either insoluble or soluble within the liquid substrate.

For the cases where the monomer is insoluble in the liquid, the surface tension interaction between the polymer and the liquid is the key parameter that determines the morphology of the deposited polymer at the vapor-liquid interface. We investigated the effect of surface tension by studying the deposition of six different polymers of varying surface tensions onto seven different liquids. Our data showed that the spreading coefficient (S) dictates the final polymer morphology at the vapor-liquid interface.[54] The spreading coefficient of low surface energy materials is defined as:

$$S = \gamma_{LV} * (1 + cos\theta_A) - 2\gamma_{PV}$$

where γ_{LV} is the surface tension of the liquid, γ_{PV} is the surface tension of the polymer, and θ_A is the advancing contact angle of the liquid on the polymer.[62] When the spreading coefficient is positive, it is energetically favorable for the polymer to spread over the liquid surface which results in a polymer film. When the spreading coefficient is negative, it is energetically favorable for the polymer to aggregate on the liquid surface which results in polymer particles. For example, the surface tension of the fluoropolymer PPFDA is low (13.6 mN/m) and a polymer film formed on all liquids tested due to a positive spreading coefficient. These liquids had a range of surface tensions from 22.8 mN/m for silicone oil to 63.4 mN/m for glycerol. In the next two sections, we

will discuss the different structures that can be formed for systems with negative spreading coefficients[54,55,58,59] and positive spreading coefficients[45,54,63] as shown in Figure 2. In addition to surface tension and solubility, we will also discuss how the viscosity of the liquid substrate affects the diffusivity of the polymer chains on the liquid surface, and thereby affects the final morphology of the structure.[54,55,57,58]

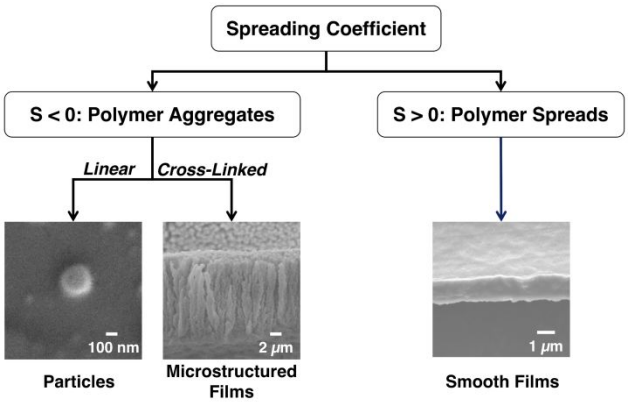

Figure 2 – The spreading coefficient determines whether polymer aggregation or polymer spreading is more energetically favorable.

Polymer Particles

If the monomer is insoluble in the liquid and the spreading coefficient is negative, the polymer chains will aggregate to form particles.[54,57,59,64] These polymer particles can either remain at the vapor-liquid interface or submerge into the bulk liquid which is determined by the Gibbs free energy of particle detachment from the vapor-liquid interface (ΔG):

$$\Delta G = -\pi r^2 \gamma_{LV} (1 - cos\theta)^2$$

where r is the radius of the particle and θ is the equilibrium contact angle of the liquid on the polymer.[65] The particle will remain at the vapor-liquid interface if the contact angle of the liquid

on the polymer is nonzero whereas the particle will submerge into the bulk if the contact angle is zero (complete wetting) (Figure 3).

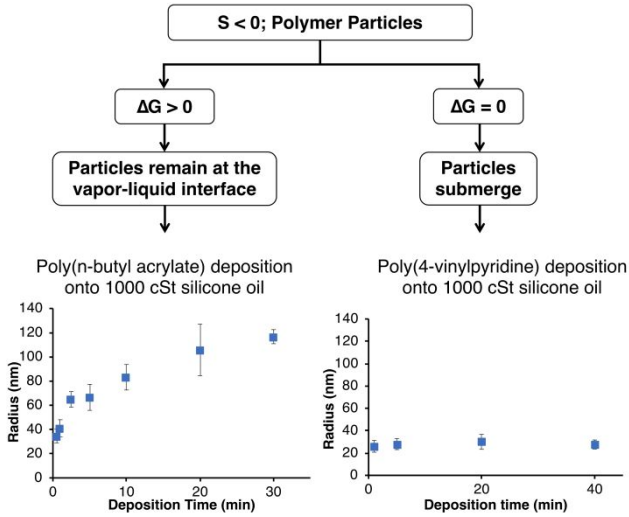

Figure 3 – Particles can either remain at the vapor-liquid interface or submerge within the bulk which depends on the Gibbs free-energy.

For example, the deposition of poly(n-butyl acrylate) (PnBA) onto silicone oil leads to the formation of polymer particles since the system has a negative spreading coefficient. Since the silicone oil has a contact angle of 21° on PnBA, the PnBA particles remain at the vapor-liquid interface and the particle size increases with deposition time as shown in Figure 3. The location of the particles at the vapor-liquid interface was confirmed by PnBA deposition onto uncured polydimethylsiloxane (PDMS) which was then cured and imaged via SEM.[59] Our systematic studies of PnBA deposition onto a range of silicone oils of different viscosities (100, 500, and 1000 cSt) showed that the growth of the particles follows a two-stage mechanism where the particles first nucleate and then newly deposited chains aggregate to the existing particles.[57] We showed that the polymer radius increased proportionally to the cubed root of the deposition time at each silicone oil viscosity as expected for the two-stage mechanism. Increasing the viscosity of the silicone oil decreases the diffusion of the polymer chains at the vapor-liquid interface, and

therefore the PnBA nanoparticles were smaller at higher viscosities at a given deposition time and deposition rate. For example, the average radii of the particles at a deposition time of 10 min and a deposition rate of 30 nm/min were 188 ± 14 nm, 106 ± 11 nm, and 83 ± 11 nm at viscosities of 100, 500, and 1000 cSt, respectively. Since the nanoparticles exhibited a two-stage mechanism, we were able to create core-shell nanoparticles by coating the PnBA particles with the light-responsive polymer poly(*o*-nitrobenzyl methacrylate), which upon exposure to UV-light transforms into poly(methacrylic acid) (PMAA). The PMAA shell can be removed in pH 8 buffer to reveal the original PnBA core.[57]

The deposition of PHEMA and poly(4-vinylpyridine) (P4VP) onto silicone oil also leads to the formation of polymer particles since these systems also have negative spreading coefficients. However, in contrast to the PnBA system, the PHEMA and P4VP particles detach from the silicone oil interface and submerge into the bulk since the silicone oil completely wets PHEMA and P4VP. The location of these particles within the bulk was confirmed by imaging cross-sections of PDMS as described above.[59] The size of these particles do not increase with time because the additional polymer deposited at the vapor-liquid interface does not aggregate with the submerged particles (Figure 3). In the iCVD process, the partial pressure of the monomer (P_m) is less than the saturation pressure of the monomer (P_{sat}) ($P_m/P_{sat} < 1$). When P4VP polymer is deposited onto 100 cSt silicone oil at P_m/P_{sat} of 0.3 for 15 min, the average radius is 137 nm ± 14 nm.[58] We recently demonstrated that we can create polymer particles with a larger average radius (233 nm ± 70 nm) by increasing the monomer partial pressure above its saturation pressure ($P_m/P_{sat} > 1$).[58] The monomer droplets condense onto the liquid surface and then submerge within the bulk liquid where they undergo coalescence and are subsequently polymerized. The coalescence results in a

broader particle size distribution and a larger average particle size as compared to polymer depositions at $P_m/P_{sat} < 1$ (Figure 4).

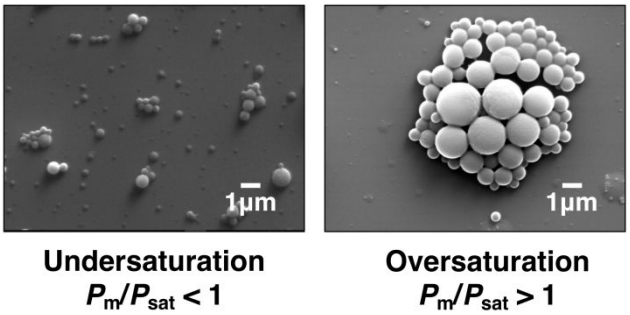

Figure 4 – The average radius of submerging polymer particles can be increased by operating at a monomer partial pressure above the monomer saturation pressure.

Polymer Films

If the monomer is insoluble in the liquid and the spreading coefficient is positive, the polymer chains will spread to form a film. For example, the low surface energy fluoropolymer PPFDA has a positive spreading coefficient on all of the ILs and silicone oils we tested and therefore a dense film always forms at the vapor-liquid interface.[54,64] If we incorporate a crosslinker, such as ethylene glycol diacrylate (EGDA), we can create mechanically robust polymer films of poly(1*H*,1*H*,2*H*,2*H*-perfluorodecyl acrylate-co-ethylene glycol diacrylate) [P(PFDA-co-EGDA)]. We showed the utility of these robust films by fabricating polymer canopies over micropillar arrays (Figure 5).[63] The canopies were fabricated by using either silicone oils or ILs as a physical mask to control the location of polymerization along the height of the pillars. The P(PFDA-co-EGDA) coating can also be used to encapsulate IL droplets using the concept of liquid marbles.[56] Millimeter-sized droplets of 1-ethyl-3-methylimidazolium tetrafluoroborate [emim][BF_4] were rolled on a bed of micron-sized PTFE particles to form the liquid marbles which were then coated within a P(PFDA-co-EGDA) shell. The PTFE particles were incorporated into

the P(PFDA-co-EGDA) polymer shell, enhancing the mechanical strength of the coating (Figure 5).

The deposition of poly(ethylene glycol diacrylate) (PEGDA) on its own onto silicone oil should lead to polymer particles because of the negative spreading coefficient (S = -56 mN/m), however a crosslinked microstructured polymer film forms due to the ability of EGDA to form crosslinks which allows for bridging of the polymer chains.[55] The microstructured PEGDA films are composed of coral-like features that form because the polymer is favorably wetted by the silicone oil as it forms the crosslinked network. Since diffusion and aggregation play key roles in the formation of the microstructured film, the viscosity of the silicone oil impacts the surface roughness of the films. Increasing the viscosity of the silicone oil leads to slower diffusion and aggregation of the polymer chains which can be quantified by a decrease in the root-mean-squared surface roughness from ~425 nm to ~150 nm for 10 cSt and 500 cSt, respectively. We also showed that polymers that have a negative spreading coefficient can be crosslinked via copolymerization with EGDA to form similar microstructured films. For example, 1-vinyl-2-pyrrolidone (VP) and HEMA were copolymerized with EGDA to form microstructured films of P(VP-co-EGDA) and P(HEMA-co-EGDA) although the spreading coefficient values are -63 mN/m and -58 mN/m on silicone oil respectively.

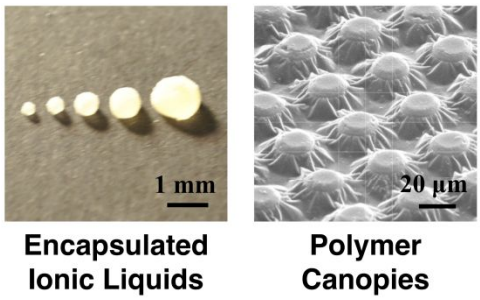

Figure 5 –Polymer films can be used to encapsulate ionic liquids or to form polymer canopies over pillared arrays.

Polymerization within the bulk

For cases where the monomer is soluble within the liquid, the liquid gets incorporated within the polymer structure. For example, HEMA is soluble in [emim][BF_4] and polymerization leads to the formation of a gel due to the ability of PHEMA to form hydrogen bonds with the IL.[23,66] Polymerization of HEMA occurs both at the vapor-liquid interface and within the IL leading to a bimodal distribution in molecular weight.[8] For example, at a reactor pressure of 80 mTorr, deposition rate of 4 nm/min, and deposition time of 5 min, the average molecular weight of the PHEMA chains formed at the vapor-liquid interface was 1.8 x 10^4 Da with a PDI of 1.7 whereas the average molecular weight of the PHEMA chains formed within the IL was 1.2 x 10^7 Da with a PDI of 1.8. The higher molecular weight of the chains formed within the IL is likely due to the higher propagation rates and reduced termination rates which is consistent with solution-phase polymerization within ILs.[25,67] We also demonstrated that we could control the shape of the gel by polymerizing HEMA within spherical droplets of [emim][BF_4].[68] The IL droplets were kept spherical by placement on a rough hydrophobic surface. Monomer was then absorbed into the droplets and then the free radicals were generated afterward to initiate the polymerization process. By sequentially introducing the monomer and initiator radicals, surface polymerization was reduced which retained the hydrophobicity of the rough surface, maintaining the spherical shape of the gels. We can also fabricate thin free-standing gels by polymerizing HEMA on a layer of IL that is surrounded by a layer of silicone oil.[64] A gel forms on the IL because HEMA is soluble whereas PHEMA particles form on the surrounding silicone oil because HEMA is insoluble. The silicone oil prevents the gel from being attached to the underlying silicon wafer and therefore the gel can be easily removed from the IL surface with tweezers.

We have also shown that IL can be incorporated into copolymer films by studying the sequential and simultaneous polymerization of EGDA and PFDA onto [emim][BF_4].[60] EGDA is soluble in [emim][BF_4], and therefore can absorb and polymerize in the bulk liquid, however PFDA is insoluble in the IL and only polymerizes at the vapor-liquid interface. In the case of simultaneous polymerization of both monomers, a heterogenous film was formed. The top layer of the film was composed of P(PFDA-co-EGDA) copolymer formed at the vapor-liquid interface whereas the bottom layer was composed of both PEGDA and IL (PEGDA+IL) due to absorption of the EGDA monomer and subsequent bulk polymerization. An unexpected result occurred in the case of sequential deposition where first a layer of PPFDA was deposited onto the IL and then a layer of PEGDA was deposited onto the PPFDA. A PEGDA layer formed on top of the PPFDA layer as expected but interestingly, a PEGDA+IL layer was formed beneath the PPFDA layer indicating that the EGDA monomer and initiator radicals can diffuse through the dense PPFDA layer and absorbs into the IL. In the PEGDA+IL bottom layer, the ionic liquid is incorporated into the PEGDA layer through the entrapment of IL between the polymer chains formed in the bulk.

In all our previous examples, the liquid substrate does not covalently bond with the monomer. We can create covalent bonds between the liquid and monomer by using a polymerizable ionic liquid such as 1-ethyl-3-vinylimidazolium bis(trifluoromethylsulfonyl)imide ([EVIm][TFSI]), which contains a vinyl bond that can be copolymerized with EGDA monomer.[61] Since EGDA is soluble in [EVIm][TFSI], it can be polymerized both within the liquid and at the vapor-liquid interface. This results in a gradient film with a PEGDA top layer and a poly([EVIm][TFSI]-co-EGDA) bottom layer. The deposition time and reactor pressure affect the IL concentration in the poly([EVIm][TFSI]-co-EGDA) copolymer layer because the growth of the

PEGDA layer at the vapor-liquid interface reduces the flux of additional EGDA and initiator into the bulk liquid. We showed that these gradient films can be formed over wire meshes for additional stability for potential applications in separations, ion conducting membranes, and catalysis.[61]

Concluding Remarks

Our studies have demonstrated the effects of surface tension and viscosity during iCVD onto liquid substrates. In order to understand whether these relationships govern the deposition of materials during other vapor phase deposition processes, we recently studied DC magnetron sputter deposition of gold and silver onto a variety of liquids of different viscosities and surface tensions.[30] We found that the trends were analogous to polymer deposition since metal sputtered onto low viscosity silicone oils ($\leq$ 100 cSt) and ILs formed nanoparticle dispersions, whereas metal sputtered onto high viscosity silicone oils ($\geq$ 350 cSt) formed films. Since the trends in iCVD and sputtering onto liquid substrates are similar, we were able to combine these two processes to create unique organic/inorganic hybrid materials.[53] For example, we fabricated polymer nanoparticles decorated with metal nanoparticles using a submerging polymer particle system. We also fabricated a gel with embedded nanoparticles using a soluble monomer-IL system. In the above examples, there is passive motion during deposition due to diffusion and surface tension effects. We recently demonstrated that we can introduce active motion by modifying the iCVD reactor with a speaker to produce standing waves on the liquid surface.[69] Our studies showed that crosslinking was required to form continuous films on the agitated vapor-liquid interface and the mechanical stability of the films can be enhanced by increasing the film thickness. Our understanding of interactions at the vapor-liquid interface during inorganic and organic deposition and our ability to actively modulate the liquid surface can enable the development of a new generation of hybrid reactors with *in situ* capabilities.

References

1 M. E. Alf, A. Asatekin, M. C. Barr, S. H. Baxamusa, H. Chelawat, G. Ozaydin-Ince, C. D. Petruczok, R. Sreenivasan, W. E. Tenhaeff, N. J. Trujillo, S. Vaddiraju, J. Xu and K. K. Gleason, *Adv. Mater.*, 2010, **22**, 1993–2027.

2 W. E. Tenhaeff and K. K. Gleason, *Adv. Funct. Mater.*, 2008, **18**, 979–992.

3 S. Seidel, C. Riche and M. Gupta, in *Encyclopedia of Polymer Science and Technology*, John Wiley & Sons, Inc., 2011.

4 K. K. S. Lau and K. K. Gleason, *Macromolecules*, 2006, **39**, 3688–3694.

5 K. K. S. Lau and K. K. Gleason, *Macromolecules*, 2006, **39**, 3695–3703.

6 G. Ozaydin-Ince and K. K. Gleason, *J. Vac. Sci. Technol. A Vacuum, Surfaces, Film.*, 2009, **27**, 1135.

7 M. Gupta and K. K. Gleason, *Langmuir*, 2006, **22**, 10047–10052.

8 R. J. Frank-Finney, L. C. Bradley and M. Gupta, *Macromolecules*, 2013, **46**, 6852–6857.

9 R. K. Bose and K. K. S. Lau, *Biomacromolecules*, 2010, **11**, 2116–2122.

10 S. H. Baxamusa and K. K. Gleason, *Chem. Vap. Depos.*, 2008, **14**, 313–318.

11 M. Gupta and K. K. Gleason, *Thin Solid Films*, 2009, **517**, 3547–3550.

12 J. Xu and K. K. Gleason, *ACS Appl. Mater. Interfaces*, 2011, **3**, 2410–2416.

13 B. Chen, P. Kwong and M. Gupta, *ACS Appl. Mater. Interfaces*, 2013, **5**, 12701–12707.

14 P. Kwong, C. A. Flowers and M. Gupta, *Langmuir*, 2011, **27**, 10634–10641.

15 P. Kwong and M. Gupta, *Anal. Chem.*, 2012, **84**, 10129–10135.

16 M. Gupta, V. Kapur, N. M. Pinkerton and K. K. Gleason, *Chem. Mater.*, 2008, **20**, 1646–1651.

17 A. Asatekin and K. K. Gleason, *Nano Lett.*, 2011, **11**, 677–686.

18 R. Yang and K. K. Gleason, *Langmuir*, 2012, **28**, 12266–74.

19 Y. Ye, Y. Mao, F. Wang, H. Lu, L. Qu and L. Dai, *J. Mater. Chem.*, 2011, **21**, 837–842.

20 E. D. Laird, R. K. Bose, W. Wang, K. K. S. Lau and C. Y. Li, *Macromol. Rapid Commun.*, 2013, **34**, 251–256.

21 C. T. Riche, B. C. Marin, N. Malmstadt and M. Gupta, *Lab Chip*, 2011, **11**, 3049–52.

22 C. T. Riche, C. Zhang, M. Gupta and N. Malmstadt, *Lab Chip*, 2014, **14**, 1834–41.

23 T. Ueki and M. Watanabe, *Bull. Chem. Soc. Jpn.*, 2012, **85**, 33–50.

24 P. C. Marr and A. C. Marr, *Green Chem.*, 2015, 18, 105–128.

25 P. Kubisa, *Prog. Polym. Sci.*, 2004, **29**, 3–12.

26 J. P. Xie, W. Y. Yu, S. L. Zhang, M. G. Chen and G. X. Ye, *Phys. Lett. A*, 2007, **371**, 160–164.

27 M. Wagener and B. Günther, *J. Magn. Magn. Mater.*, 1999, **201**, 41–44.

28 D. Sugioka, T. Kameyama, S. Kuwabata and T. Torimoto, *Phys. Chem. Chem. Phys.*, 2015, **17**, 13150–13159.

29 H. Wender, L. F. De Oliveira, P. Migowski, A. F. Feil, E. Lissner, M. H. G. Prechtl, S. R. Teixeira and J. Dupont, *J. Phys. Chem. C*, 2010, **114**, 11764–11768.

30 M. M. De Luna and M. Gupta, *Appl. Phys. Lett.*, 2018, **112**, 201605.

31 C. Feng, H. Ge, M. Tong, G. Ye and Z. Jiao, *Thin Solid Films*, 1999, **342**, 30–34.

32 E. F. Borra, O. Seddiki, R. Angel, D. Eisenstein, P. Hickson, K. R. Seddon and S. P. Worden, *Nature*, 2007, **447**, 979–981.

33 G. Ye, Q. Zhang, C. Feng, H. Ge and Z. Jiao, *Phys. Rev. B*, 1996, **54**, 14754–14757.

34 P. Cai, S. Yu, X. Xu, M. Chen, C. Sui and G. X. Ye, *Appl. Surf. Sci.*, 2009, **255**, 8352–8358.

35 M.-G. Chen, J.-P. Xie and G.-X. Ye, *Phys. Lett. A*, 2006, **360**, 323–326.

36 B. Yang, R.-R. Ma, D.-M. Li, A.-G. Xia and X.-M. Tao, *Thin Solid Films*, 2012, **520**, 2321–2325.

37 T. Torimoto, K. I. Okazaki, T. Kiyama, K. Hirahara, N. Tanaka and S. Kuwabata, *Appl. Phys. Lett.*, 2006, **89**, 243117.

38 Y. Hatakeyama, T. Morita, S. Takahashi, K. Onishi and K. Nishikawa, *J. Phys. Chem. C*, 2011, **115**, 3279–3285.

39 Y. Hatakeyama, K. Onishi and K. Nishikawa, *RSC Adv.*, 2011, **1**, 1815–1821.

40 C.-H. Liu, B.-H. Mao, J. Gao, S. Zhang, X. Gao, Z. Liu, S.-T. Lee, X.-H. Sun and S.-D. Wang, *Carbon N. Y.*, 2012, **50**, 3008–3014.

41 K. Ueno and H. Misawa, *J. Photochem. Photobiol. C Photochem. Rev.*, 2013, **15**, 31–52.

42 N. Binh-Khiem, K. Matsumoto and I. Shimoyama, *Langmuir*, 2010, **26**, 18771–18775.

43 J. T. Wu, C. Y. Wu, S. K. Fan, C. C. Hsieh, Y. C. Hou and H. Y. Chen, *Chem. Mater.*, 2015, **27**, 7028–7033.

44 N. Binh-Khiem, K. Matsumoto and I. Shimoyama, *Appl. Phys. Lett.*, 2008, **93**, 2006–2009.

45 P. D. Haller, R. J. Frank-Finney and M. Gupta, *Macromolecules*, 2011, **44**, 2653–2659.

46 G. Vilar, J. Tulla-Puche and F. Albericio, *Curr. Drug Deliv.*, 2012, **9**, 367–94.

47 S. Pathak, M. T. Greci, R. C. Kwong, K. Mercado, G. K. S. Prakash, G. A. Olah and M. E. Thompson, *Chem. Mater.*, 2000, **12**, 1985–1989.

48 Y. Shi, M. Wang, C. Ma, Y. Wang, X. Li and G. Yu, *Nano Lett.*, 2015, **15**, 6276–6281.

49 G. Ruan, G. Vieira, T. Henighan, A. Chen, D. Thakur, R. Sooryakumar and J. O. Winter, *Nano Lett.*, 2010, **10**, 2220–2224.

50 L. L. Chng, N. Erathodiyil and J. Y. Ying, *Acc. Chem. Res.*, 2013, **46**, 1825–1837.

51 A. Dokoutchaev, J. Thomas James, S. C. Koene, S. Pathak, G. K. Surya Prakash and M.

E. Thompson, *Chem. Mater.*, 1999, **11**, 2389–2399.

52 W. Li, Q. Liu and L. Liu, *Langmuir*, 2014, **30**, 12619–26.

53 M. M. De Luna, P. Karandikar and M. Gupta, *ACS Appl. Nano Mater.*, 2018, **1**, 6575–6579.

54 P. D. Haller, L. C. Bradley and M. Gupta, *Langmuir*, 2013, **29**, 11640–11645.

55 L. C. Bradley and M. Gupta, *Langmuir*, 2015, **31**, 7999–8005.

56 L. C. Bradley and M. Gupta, *Langmuir*, 2012, **28**, 10276–10280.

57 R. J. Frank-Finney and M. Gupta, *Langmuir*, 2016, **32**, 11014–11020.

58 P. Karandikar and M. Gupta, *Langmuir*, 2017, **33**, 7701–7707.

59 P. D. Haller and M. Gupta, *Macromol. Rapid Commun.*, 2014, **35**, 2000–2004.

60 L. C. Bradley and M. Gupta, *Langmuir*, 2013, **29**, 10448–10454.

61 L. C. Bradley and M. Gupta, *Macromolecules*, 2014, **47**, 6657–6663.

62 H. W. Fox and W. A. Zisman, *J. Colloid Sci.*, 1952, **7**, 109–121.

63 B. Chen, R. J. Frank-Finney and M. Gupta, *ACS Appl. Mater. Interfaces*, 2015, **7**, 23056–23061.

64 R. J. Frank-Finney, P. D. Haller and M. Gupta, *Macromolecules*, 2012, **45**, 165–170.

65 S. E. Anachkov, I. Lesov, M. Zanini, P. A. Kralchevsky, N. D. Denkov and L. Isa, *Soft Matter*, 2016, **12**, 7632–7643.

66 Z. Li, H. Liu, Y. Liu, P. He, J. Li, L. Zheng and J. Li, *Polymer*, 2005, **46**, 7578–7584.

67 S. Harrisson, S. R. Mackenzie and D. M. Haddleton, *Macromolecules*, 2003, **36**, 5072–5075.

68 P. Karandikar and M. Gupta, *Thin Solid Films*, 2017, **635**, 17–22.

69 P. Karandikar, M. M. De Luna and M. Gupta, *ACS Appl. Polym. Mater.*, 2019, 10.1021/acsapm.9b00256.